THESIS FOR THE DEGREE OF LICENTIATE OF ENGINEERING

THE COMPOSITE CYCLE ENGINE: PERFORMANCE AND EMISSIONS

ADAM JOHANSSON

Department of Mechanical Engineering
CHALMERS UNIVERSITY OF TECHNOLOGY
Göteborg, Sweden 2026

The Composite Cycle Engine: Performance and Emissions
ADAM JOHANSSON

Department of Mechanical Engineering
Chalmers University of Technology
SE-412 96 Göteborg, Sweden
Telephone +46 (0)31 772 10 00

Cover: Rendering of the concept of an intercooled composite cycle engine.

Chalmers digitaltryck
Göteborg, Sweden 2026

The Composite Cycle Engine: Performance and Emissions

ADAM JOHANSSON
Department of Mechanical Engineering
Chalmers University of Technology

Abstract

Currently, there is no viable solution to decarbonise aviation. It is therefore of outmost importance to develop the most fuel efficient engines possible. Current aero engines are reaching the technological limit of thermal efficiency, where further development yields diminishing returns. A novel type of propulsion system is the composite cycle engine that offers fuel burn reductions beyond what is possible with a conventional turbofan design. The rationale for the concept is to replace the turbomachinery and combustor in the high-pressure part of a turbofan with a piston engine. Combustion inside a piston engine is more efficient than a constant pressure burner, resulting in a higher overall efficiency of the propulsion system. Unfortunately, it also leads to higher emissions of nitrogen oxides (NO_x). This thesis presents a framework for the thermodynamic modelling of the composite cycle engine together with a methodology to assess emissions of NO_x. The developed framework enables design studies of the engine, where performance and emissions can be analysed. A parametric study is presented where the impact of key thermodynamic cycle design variables on efficiency, power density, and NO_x is investigated. Prohibitive levels of NO_x were found for all the parameters studied. Finally, an outlook for further work using the developed model is discussed, with possible techniques to reduce NO_x.

Keywords: composite cycle engine, thermal efficiency, nitrogen oxides, aero engine, piston engine, turbofan, joule cycle, climate impact

Författarens tack

Först och främst vill jag tacka min handledare Carlos för din hjälp och vägledning. Ibland kan jobbet kännas tufft, men den känslan är alltid som bortblåst efter att jag har pratat med dig. Tack också till min bihandledare Anders, som alltid varit inspirerande och bidragit med otroligt mycket kunskap. Jag vill också tacka alla trevliga kollegor på avdelningen, det är de små pratstunderna i fikarummet eller korridoren som gör det så kul att gå till jobbet. Speciellt tack till Niklas för alla löptips och Srdjan för alla intressanta samtal om historia och politik. Ett extra tack till alla jag delar kontor med, jag kan inte tänka mig bättre kontorsgrannar, även om vi ibland kanske har lite för roligt för jobbets bästa. Nu till New Yorkshire Cityjaure, ni är de bästa vännerna man kan tänka sig. Att vi alla valde att stanna på Chalmers och doktorera känns ibland för bra för att vara sant. Här vill jag även tacka Kårrestaurangen för alla utsökta luncher. Tack till alla mina andra vänner som antagligen aldrig kommer att läsa detta, det är skönt att komma ut ur Chalmersbubblan ibland och se den riktiga världen. Tack till släkten, ni är alltid där för mig. Väldigt roligt att gå i både farfars, pappas och Annas fotspår på Chalmers. Det är du farfar som väckte mitt intresse för både kolvmotorer och flygmotorer. Tack till morfar, jag önskar att du fortfarande var med oss. Slutligen till familjen: tack för att ni är bäst. Alltid skönt att kunna prata om doktorerandet med dig, pappa, och tack för alla Bulten-häng, Ellen. Mamma, tack för allt egentligen, det finns ingenting du inte gör för mig. Slutligen tack till dig Ellinor, att jag har träffat dig är det bästa som hänt mig.

Adam Johansson
Göteborg, januari 2026

List of Appended Papers

This thesis is based on work presented in the following papers:

I **Modelling a hydrogen fuelled composite cycle aero engine**
Adam Johansson, Petter Miltén, Anders Lundbladh, Carlos Xisto
In proceedings of the 34th Congress of the International Council of the Aeronautical Sciences, Florence, Italy, 2024.

II **Performance and NOx emission characteristics of intercooled composite cycle aero engines**
Adam Johansson, Anders Lundbladh, Tomas Grönstedt and Carlos Xisto
To be submitted to Aerospace Science and Technology, 2026.

Contents

List of abbreviations

BPR bypass ratio. 4, 11, 13

CCE composite cycle engine. 5, 6, 15, 19, 21, 23, 31–34

ERF effective radiative forcing. 2

HPC high-pressure compressor. 11, 17, 19

HPT high-pressure turbine. 11, 17

LPC low-pressure compressor. 11, 17, 18

LPT low-pressure turbine. 11

OHC oxygen-hydrogen-carbon. 29, 31

OPR Overall Pressure Ratio. 13, 33

TIT turbine inlet temperature. 12, 13

ToA top-of-the-atmosphere. 2

1 Introduction

We are in a time where the global emissions of greenhouse gases are still reaching record levels and the effects of global warming are already clearly visible. There is a consensus that greenhouse gas emissions from human activities need to decrease, but the way forward is not clear. However, positive signs can be seen and renewable energy sources are expected to produce more electricity globally than coal in 2025 for the first time [1]. Furthermore, in the first three quarters of 2025, the increase in solar and wind power outpaced the growth in global electricity demand [2]. Many industries have a technical solution for decarbonisation that is already available. For example, road transport can be electrified, power generation can be achieved with renewable energy, and building heating can be decarbonised through the use of heat pumps and improved energy efficiency. However, one industry still lacks any viable decarbonisation solution: aviation.

With this background, it is clear that all possible technical solutions to achieve carbon neutrality in aviation need to be researched. In this introduction, the climate impact of aviation will be presented. Thereafter, a summary of previous and ongoing research activities on climate friendly aircraft propulsion will be put forward. Finally, the purpose of this individual work will be described, followed by a presentation of the structure of the thesis.

1.1 Climate impact of aviation

Aviation accounts for approximately 3.5% of net anthropogenic climate change [3]. However, this fraction is expected to grow since many other transport industries are reducing their climate impact, while aviation is growing and difficult to decarbonise. The Earth's surface is warmed by global aviation both from carbon dioxide (CO_2) and non-CO_2 contributions, with the distribution of the three most important contributors shown

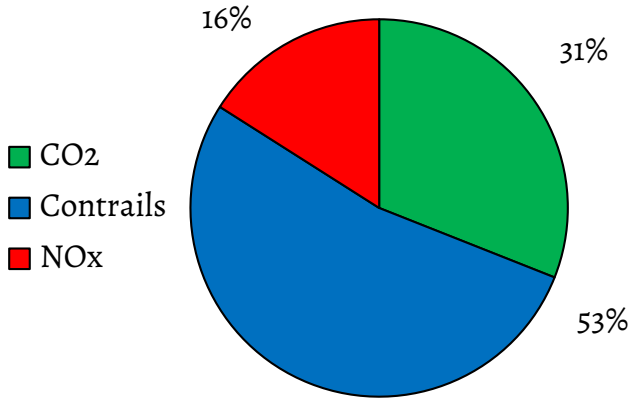

Figure 1.1: Effective radiative forcing distribution of global aviation in 2018. Adapted from [3].

in Fig. 1.1. Approximately 53% of the effective radiative forcing (ERF) is from contrails, 16% from nitrogen oxide NO_x emissions, and 31% from CO_2. Interestingly, non-CO_2 effects comprise about two thirds of the total net effective radiative forcing, although these effects are associated with significant uncertainties.

ERF is the key metric for assessing the influence of natural and human contributions to climate change[4]. It extends the concept of radiative forcing, which measures the instantaneous change in Earth's radiative flux at the top-of-the-atmosphere (ToA) due to a perturbation. However, the release and change of concentration of different greenhouse gases can lead to a rapid atmospheric response, further affecting the radiation balance, which is not captured by the radiative forcing metric. Therefore, ERF represents the change in radiative flux at the ToA after rapid adjustment of clouds, water vapour, and atmospheric temperature, but with constant surface temperatures at land and sea.

The climate effect of CO_2 is long lived as CO_2 remains in the atmosphere for centuries [5]. Contrail cirrus and NO_x on the other hand create short lived radiative forces and are associated with larger uncertainties. A short-term effect of NO_x emissions is an increase in tropospheric ozone, which is a greenhouse gas. In the long-term, it leads to a depletion of methane, a powerful greenhouse gas. Hence, there is a warming and cooling effect caused by the NO_x emissions. However, since continuously more NO_x is emitted into the atmosphere, the short-term effect dominates and the contribution to global warming has increased. When the ambient atmosphere through which the aeroplane flies is supersaturated with respect to ice, the exhaust of the engines produces persistent condensation trails (contrails), which could lead to cloudiness that would not appear otherwise. These cirrus clouds can have both cooling and warming effects. During the night, the effect is exclusively warming. Estimating the net global effect is a

complex task, but the best estimate, including uncertainties, is that the contrail cirrus is warming.

1.2 Climate friendlier aviation

The reason for the challenge of decarbonising aviation is due to its high energy-intensity, while at the same time being weight sensitive [6]. Except for very short ranges and low capacities, the main source of energy for propulsion will probably be liquid fuels for the first half of the century [7]. Electric batteries are simply too heavy for short to long range flights that are today covered by single-aisle and twin-aisle jet powered aircraft. For example, the originally proposed Heart Aerospace 19 seat electric plane ES-19 had a predicted range of 400 km [8]. They have now moved on to a hybrid concept instead. Consequently, the most probable way to decarbonise air travel is to switch from fossil fuels to bio-fuels or electro-fuels [9]. However, these fuels are resource-intensive, with electro-fuels that have a fairly poor efficiency from electricity to fuel energy, and bio-fuels that require a large use of land, potentially competing with food production [10] [11]. In economic terms, the cost of these energy carriers will be higher than that of fossil fuels today [12]. Therefore, these fuels must be used in the most efficient manner possible. In other words, highly efficient propulsion systems and aircraft will be extremely important to realise a cost effective and sustainable future in aviation.

The most obvious way to reduce global aviation fuel consumption is by reducing air traffic. In 2020, global air travel emissions were reduced by 40% due to the COVID-19 pandemic. However, it is expected that the demand for air traffic will recover and grow further [10]. Historically, the energy intensity of air travel, provided in terms of energy per passenger kilometre, has declined by 60% between 1970 and 2021, at an average of 1% per year [10]. This can be largely attributed to the introduction of widebody aircraft in the 1970s, the introduction of high bypass turbofans, and the continued introduction of fuel-efficient narrowbody and small widebody planes [13]. From 1959 to 1995, 57% of the reduction in energy intensity can be attributed to engine improvements, 22% to aerodynamic improvements, 17% to increased load factor of passengers and 4% to higher seating capacity [14]. Aerodynamic efficiency was primary driven by improved wing design and engine integration. As can be seen, there are multiple ways to reduce the energy intensity, with the improvement of the propulsive system being the most important historically. In this thesis, we focus only on how the engine can achieve a further reduction in energy consumption.

The overall efficiency of the propulsion system can be divided into thermal efficiency and propulsive efficiency. Thermal efficiency is the fraction of fuel energy that is converted into kinetic energy of the gas stream. The efficiency with which this energy is converted into useful thrust is measured by the propulsive efficiency. This concept is explained in more detail in Chapter 2.

Propulsive efficiency is improved by reducing the outlet velocity of the propelled gas. For turbofan engines, this is achieved by dividing the engine into two parts: core and bypass. In the core, the fuel is combusted, generating power for the bypass and producing high velocity thrust. Low velocity thrust is generated in the bypass by a fan. The ratio between bypass and core mass flow is called bypass ratio (BPR) and correlates with propulsive efficiency. Starting with the Rolls-Royce Conway in 1959 [15], the BPR has increased from 0.3 to 12.5 in the modern Pratt & Whitney PW1000G engines [16], with propulsive efficiency exceeding 80% [17].

Increases in propulsive efficiency have been made possible by higher power-density and more compact engine cores, advanced engine architectures such as multi-spool designs and geared turbofans, and improvements in fan aerodynamics and lightweight materials. To achieve even higher propulsive efficiencies, research is carried out investigating concepts that go beyond the typical turbofan architecture. In [18] Kirner et al. investigated distributed propulsion. It is a concept utilising turboelectric propulsion, decoupling the power generation from the propulsive devices. This allows for distribution of relatively small propulsors along the aircraft wing span, achieving 4.1% fuel burn savings compared to a comparable aeroplane with normal propulsion.

The most promising concept that has been investigated since the 1970s is the open rotor, which removes the nacelle altogether and operates with BPRs up to 70. Currently, the CFM Rise technology demonstrator programme is in progress, with the goals of 20% reduction in fuel burn compared to current state-of-the art engines [19]. One main challenge that remains to overcome is the far-field noise, where the lack of muffling nacelle leads to higher sound levels [20]. Independently of which high-propulsive-efficiency-concept will prove to be the path forward, power must be generated in some way. In a thermal engine, the efficiency with which this power is generated from the fuel energy is quantified by thermal efficiency. Improvements in thermal efficiency are therefore universally beneficial, providing more power available for thrust generation per unit of fuel.

Improvements in thermal efficiency have been one of the main drivers of reducing fuel burn since the introduction of the jet engine. With the first operational gas turbine having a thermal efficiency of 18% [21] to today's large turbofans showing a remarkable efficiency of over 50% [17]. This progress has been driven by several factors, which I will elaborate on in Chapter 2. Worth pointing out is that the operating thermodynamic cycle, the Joule cycle, has been the same since the first jet engine. However, a point has been reached where the thermal efficiency of this cycle is projected to level out [22]. To further make the core more efficient, a new type of thermodynamic cycle is needed [23].

Various novel core concepts have been proposed. Many of them feature completely new, unproven, technology that would take a long time to develop. Since reducing global warming is an urgent matter, engine core concepts using high maturity technology are more likely to enter service and reduce climate impact sooner rather than later. A predecessor of the Horizon Europe MINIMAL project was the H2020 EU-project ULTIMATE,

where an overview and down-selection of potential future propulsion concepts was performed. They concluded that one of the most promising concepts was the composite cycle engine (CCE) [24] [17]. The CCE is a piston topping based propulsion system that combines two mature cycles for the production of gas power to drive the main propulsion system. This engine concept will be explained in detail in Chapter 3, but essentially there is a theoretical advantage of combusting the fuel inside a piston engine instead of using a conventional constant pressure burner as is done in today's jet engines.

Historically, right before the jet engine came to dominate air propulsion, the trend of larger piston engines with more turbocharging led to earlier development of composite cycle engines. Two prominent examples are the Napier Nomad [25] and the Wright R-3350 Duplex-Cyclone [26] engines.

Today, 70 years later, piston engine technology has improved significantly. Therefore, in recent years, the concept has regained attention. Early modern work includes a 1997 Rolls-Royce patent describing a CCE architecture that incorporates a rotary internal combustion engine [27]. Renewed attention was sparked by the 2013 patent for the free-double piston design by MTU Aero Engines [28].

The concept was studied in by 2016 Kaiser et al. where a comparative study between a CCE and an equivalent turbofan was performed. The results obtained reported a potential to reduce fuel burn by 15%[22]. This was followed by a study in 2018 exploring synergies between CCE, heat recuperation, and intercooling [29]. An additional 1.9% reduction in fuel burn was found from intercooling, mainly due to the reduced weight and volume of the piston engine from the higher density core air. However, due to the relative cold exhaust, recuperation was not found to be beneficial.

The most comprehensive work on the concept is the PhD thesis by Kaiser [30] published in 2020. A detailed design study was presented, where the four-stroke, two-stroke, and free-double-cylinder architectures were compared against conventional technology. For the four stroke concept, the overall efficiency was found to increase by 12.3%, but the total mission fuel burn was only reduced by 5.7% due to the increased engine weight. The two-stroke concept was found to have slightly worse thermal efficiency, but total fuel burn was reduced by another 1.1% due to the lower engine weight. Finally, the free-piston concept resulted in 15% less mission fuel burn because of a 14% improvement in overall efficiency and a relatively higher power density compared to other CCE concepts. The lower mission fuel consumption, relative to the efficiency gains, is the result of the cascade effect of carrying less fuel. Even if great fuel burn savings could be achieved, an increase in NO_x emissions was reported to increase by a factor of three.

Based on these results and the findings of ULTIMATE [17], the EU-project MINIMAL was founded. The objective of MINIMAL is, among others, to mature the concept of the CCE. Three different concepts are investigated, one based on a normal piston engine with a crankshaft, one based on the free-double-piston concept, and one on an opposed free-piston concept. These concepts will be described in Chapter 3. My contribution to the project is to further analyse the crankshaft based engine, with a focus on the emis-

sions of NO_x, since they have been found in previous studies too be high.

1.3 Purpose

It is evident that new solutions are needed to reduce the climate impact of the aviation industry. A promising concept is the composite cycle engine, which is based on mature technology and has been found to reduce mission fuel burn by at least 5.7% compared to an engine based on just continued development of the turbofan. However, the emission of NO_x from this engine would rather lead to an increased climate impact, so a solution must be found before this concept can become viable.

The purpose of my research has been to develop a modelling framework to analyse the performance and NO_x emissions of the CCE. The overarching goal is to use the model to find design trades between NO_x emissions and efficiency. Ultimately, the models should be integrated into a climate impact optimisation framework to find the engine architecture that results in the minimum climate impact.

1.4 Structure of the thesis

This thesis is structured as follows: in Chapter 2 the fundamentals of aeroplane propulsion are provided, explaining the governing equations and the working principles of modern aero engines. Chapter 3 presents the composite cycle engine, the theoretical motivation followed by the technical concepts studied in the MINIMAL project. Next, in Chapter 4, the modelling methodology that was used to analyse the CCE is presented. Finally, in Chapter 5, a summary of the work and the results is given, followed by an outlook on future research activities.

2 Aeroplane propulsion

To understand why new propulsion concepts are needed, it is useful to first review how aeroplane propulsion is currently achieved. The fundamental requirements and physical constraints of aircraft propulsion are presented first, in section 2.1. Based on that, the working principle of the dominating thrust generator, the ducted fan, is described in Section 2.2. Subsequently, Section 2.3 explains how the powerplants for these fans work. Combining the ducted fan with the gas turbine results in the turbofan architecture, of which the operation and technical limits are presented and discussed in the last section.

2.1 Fundamentals of aeroplane propulsion

For an aeroplane in flight, the acting forces can be divided into four components, see Fig. 2.1. In the vertical direction there is the gravitational force that is pulling the plane towards the ground, and is countered by an equally large lift force generated by the wings. Horizontally, there is a drag force caused by air resistance that depends on the flight speed, shape, and size of the aeroplane. The job of engines is to overcome drag by producing a propelling force, called thrust, in the direction of flight.

Aero engines produce thrust according to Newton's third law: air is ingested in the front with velocity v_a, accelerated and ejected at a higher exit momentum v_e in the exhaust, see Fig. 2.2. The net thrust, F_N, is given by :

$$F_N = \dot{m}(v_e - v_a), \tag{2.1}$$

where $\dot{m}$ is the mass flow of air accelerated by the engine. For simplicity, this expression neglects any fuel added to the mass flow and assumes that the static pressure at the

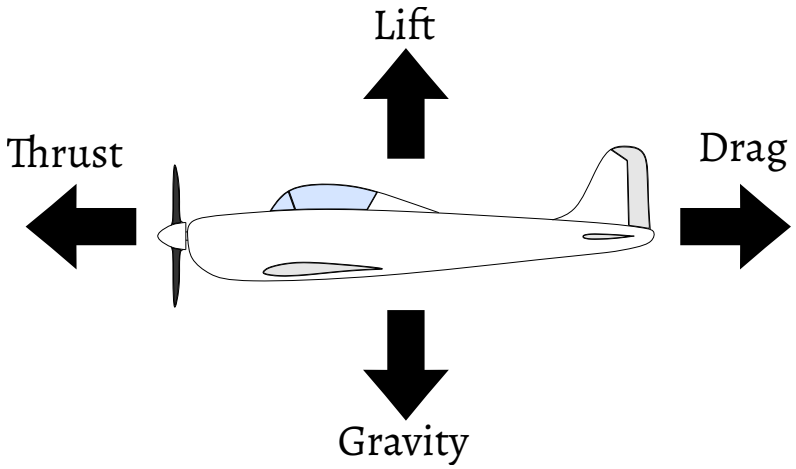

Figure 2.1: The forces acting on an aeroplane in flight. Adapted from Aircraft-diagram by Laplace42, via Wikimedia Commons, CC-BY-SA 4.0.

engine exit is equal to the ambient pressure. The increase in kinetic energy per unit of time, $\Delta \dot{W}_k$ of the air stream inside the engine is:

$$\Delta \dot{W}_k = \frac{\dot{m}}{2}(v_e^2 - v_a^2). \tag{2.2}$$

Here, the fundamental problem of propulsive efficiency is apparent. At a constant airspeed v_a, the energy needed to accelerate the air mass increases quadratically with v_e, but the thrust increases only linearly. The fraction of kinetic energy of the jet that is converted into useful thrust is called propulsive efficiency and is defined as:

$$\eta_p = \frac{F_n v_a}{\Delta \dot{W}_k} = \frac{2}{1 + \frac{v_e}{v_a}}, \tag{2.3}$$

where the product $F_n v_a$ is the propulsive power. Note that the propulsive efficiency is 100% for $v_e = v_a$, but then also $F_N = 0$. This conversion between kinetic energy and thrust is one of the major losses in the propulsion system, and the remedy is to propel larger mass flows of air at lower velocities. Practically, this is realised by larger engine diameters, which is limited by increased drag, weight, and installation issues (the engine must fit under the wing).

The other major loss is the conversion from the thermal power of the combusted fuel to the kinetic power of the air stream, and it is defined as follows:

$$\eta_{th} = \frac{\Delta \dot{W}_k}{\dot{Q}_f}, \tag{2.4}$$

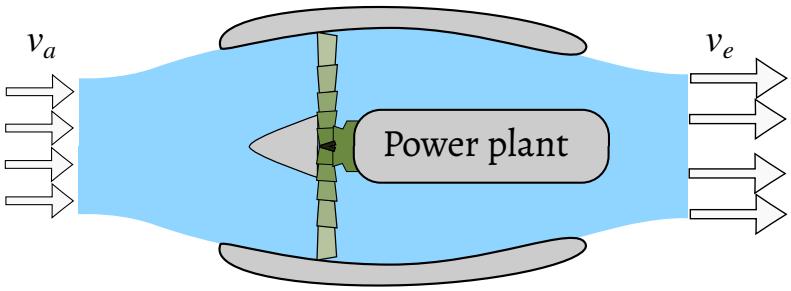

Figure 2.2: A ducted fan, the kind of aero engine powering the majority of civil aviation except short regional flights.

with $\dot{Q}_f$ being the added thermal power from the fuel. Combining the two conversion processes, we obtain the overall efficiency η_o, i.e. from fuel power to propulsive power:

$$\eta_o = \eta_{th}\eta_p = \frac{F_N v_a}{\dot{Q}_f}. \tag{2.5}$$

One of the main objectives of aero engine development is to increase η_o, both by improving η_p and η_{th}. In this thesis, we will focus on thermal efficiency, which will be explained in greater detail below. First, however, we will briefly explain the working principles behind modern aero engines.

2.2 Ducted fans

In the previous section, it was explained how thrust is produced by Newton's third law, and the two main conversion processes that affect efficiency were presented. It was seen that to achieve a high propulsive efficiency, a lowest possible velocity increase of the air was desirable. To generate enough thrust, large mass flows are needed. At the flight speeds of modern civil airlines, the best way to realise high efficiency thrust is by ducted fans. They operate by decelerating the incoming air in the intake duct, pressurising it with the large fan, and finally expanding the air in a nozzle to generate thrust. The power requirements of these fans reach up to 60 MW for large engines [31]. In Fig. 2.2 a ducted fan with a generic power plant is seen, with ambient velocity, v_a and outlet velocity, v_e shown.

In principle, any kind of power plant could be used to drive the fan. However, the weight of the engine is important, since more weight requires more lift, leading to increased drag and hence larger thrust. Therefore, a light power generator is desirable. In practice, only gas turbine engines can offer the needed power-to-weight ratio, and that is why essentially all modern aero engines are powered by gas turbine cores. When powering a ducted fan, the engine is called a turbofan.

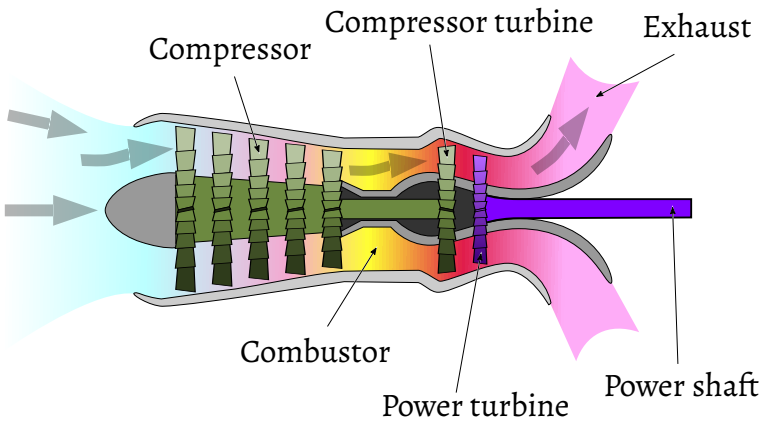

Figure 2.3: Schematic of a gas turbine engine. Adapted from Turboshaft operation by Mliu92, via Wikimedia Commons, CC-BY-SA 4.0.

2.3 Gas turbine engines

A gas turbine engine is a continuous flow internal combustion engine that converts the chemical energy of a fuel to useful work. A schematic of a gas turbine is shown in Fig. 2.3. The key component of gas turbines is the turbomachinery, which consists of compressors and turbines. In the compressor, rotating blades transfer energy from the rotor to the fluid, producing a continuous flow of pressurised gas. Inversely, in the turbine, the hot, high-pressure gas is expanded against a rotor, exerting force on the turbine blades. Torque is generated by extracting energy from the gas by decreasing its pressure and temperature and converting it into shaft work. The gas turbine works by ingesting ambient air and compressing it to a higher pressure in the compressor. Thereafter, the fuel is mixed with the air in the combustor, where it burns and raises the temperature. The hot gas expands in the first turbine, the compressor turbine, which powers the compressor. After the gas compressor turbine, there is still available energy left in the gas, which can drive a power shaft through a power turbine or be used to accelerate the gas in a nozzle.

Generally, propulsion systems designed for lower flight speeds transfer more power through the turbine, generating thrust with a propeller or fan. Systems designed for higher speeds, such as military aeroplanes, produce more thrust with the hot gas directly in the core nozzle. For civil airliners, the dominant engine type is the turbofan, where most of the power is used to drive the fan.

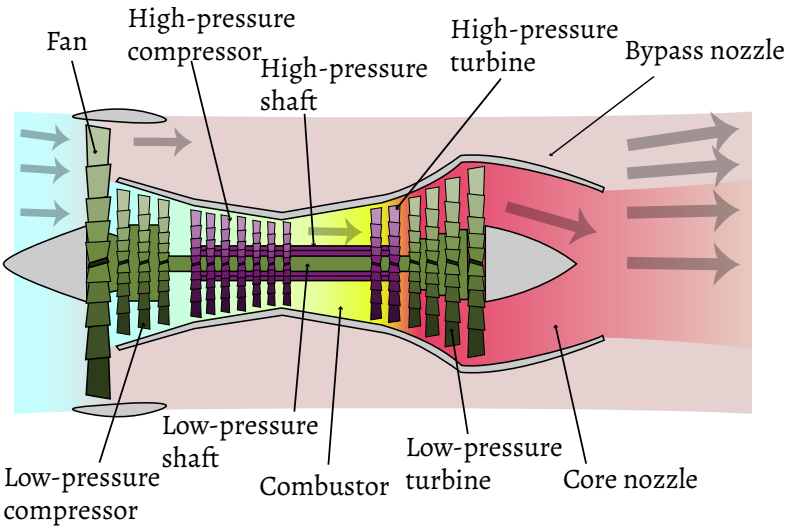

Figure 2.4: Schematic of a turbofan, with the low-pressure machinery in green and high-pressure machinery in purple. Adapted from Turbofan operation by K. Aainsqatsi, via Wikimedia Commons, CC-BY-SA 4.0.

2.4 Turbofans

Combining the ducted fan and the gas turbine results in a turbofan. This is the completely dominant engine type for the majority aviation, both civil and military, except for short regional flights. A schematic of a turbofan is shown in Fig. 2.4. The fan pressurises all of the intake air, which is then split between producing low-speed thrust in the bypass and entering the core. The ratio between the mass flow in the bypass and the core is called the bypass ratio (BPR) and is a key performance metric of the turbofan. In modern civil turbofans, more than 90% of air is flowing in the bypass, which is then used to produce most of the thrust.

Note how there are two shafts in the turbofan in Fig. 2.4, one high-pressure and one low-pressure shaft. The fan and the low-pressure compressor (LPC) are driven by the low-pressure turbine (LPT), while the high-pressure compressor (HPC) is driven by the high-pressure turbine (HPT). That is because the turbomachinery operates best at high speed, but not supersonic. Since the diameter varies between the large fan and the small stages in the high pressure compressor, the rotational speeds of the two are decoupled. In pursuit of a higher propulsive efficiency, BPR, and hence the fan diameter, is increasing. To limit the fan tip Mach number, even lower rotational speed is needed. In order for the low pressure turbine and compressor to rotate faster, a gearbox between the fan and the low-pressure shaft can be introduced. Future engines are projected to achieve even higher BPRs, and the trend is towards the full implementation of geared turbofans.

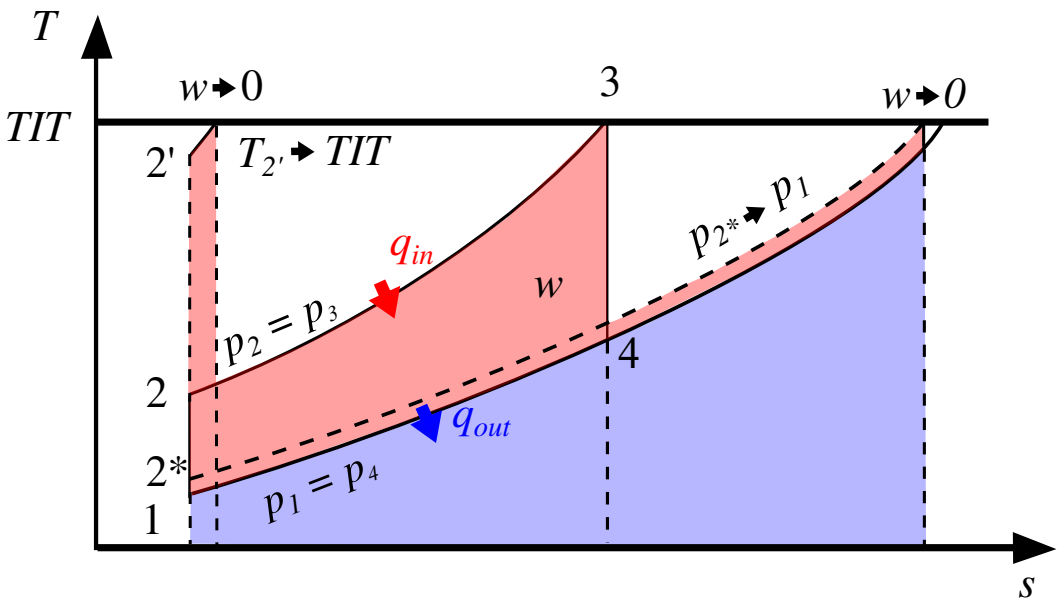

Figure 2.5: Temperature-entropy diagram of ideal Joule cycles. Specific work of the cycle, w, is represented in red shaded areas.

2.5 Joule cycle

The thermal efficiency of the entire turbofan is determined primarily by the thermal efficiency of the gas turbine engine core, except for the losses when the power is transferred from the core to the bypass air stream. The operating cycle of a gas turbine is called the Joule cycle, and a temperature-entropy (T-s) diagram of the ideal cycle is shown in Fig. 2.5. Four points connect the cycle, stations 1-4. Between 1 and 2 there is an isentropic compression, from p_1 to p_2. The combustion inside the burner is represented from 2 to 3 as the addition of heat q_{in} to the maximum cycle temperature, turbine inlet temperature (TIT), at pressure $p_2 = p_3$. The turbine is represented as an isentropic expansion from p_3 to p_4, from 3 to 4. The admission of fresh air is represented as heat rejected along the $p_1 = p_4$ isobar, with the amount q_{out}, from 4 to 1. Graphically in the T-s diagram, the amount of heat added is the area bound by the isobar between 2 and 3 and the x-axis. The amount of heat rejected is the area between the 4-1 isobar and the x-axis. The mass specific work, w, is given by:

$$w = q_{in} - q_{out} \tag{2.6}$$

which is the red area. The thermal efficiency is defined as:

$$\eta_{th} = \frac{w}{q_{in}} \tag{2.7}$$

visually represented as the ratio between the red area and the area defined by both the blue and red areas. In a T-s diagram, the slopes of the isobars increase with higher pres-

sure. Therefore, to maximise thermal efficiency, we want the ratio $r = p_2/p_1$ to be as large as possible. For an ideal Joule cycle, the thermal efficiency can be expressed as:

$$\eta_{th} = 1 - \frac{1}{\mathrm{r}^{(\gamma-1)/\gamma}}, \tag{2.8}$$

where γ is the ratio of the specific heats of the gas. However, for a fixed TIT, the specific work decreases as T_2 approaches TIT, since less heat can be added to the cycle. This is shown as the cycle with a large pressure ratio, from 1 to 2', where the temperature after compression is $T_{2'}$. Nevertheless, the cycle would have a high η_{th} since the ratio between the red and blue areas is large. In contrast, for a small r, the specific work also goes to zero, since heat must be added at increased pressure to perform the work. In the diagram this is seen in the cycle where heat is added along p_{2^*}, where the isobar almost follows the p_1 isobar. This cycle would have a low η_{th} and a low w. Consequently, for a given TIT there is an optimal r that produces the largest w.

In reality, compression and expansion are not isentropic, and η_{th} is also directly dependent on TIT. For real engines, the term Overall Pressure Ratio (OPR) is used for the pressure ratio. For each TIT, an optimal efficiency is obtained at a certain OPR, which increases with TIT. Further increasing OPR beyond its optimum results in a decrease in efficiency because increased compressor work outweighs the decrease in fuel needed to reach the required TIT, from the higher compressor outlet temperature. In addition to increasing the efficiency of individual components, which is of course extremely important, improvements to the core thermal efficiency are achieved by increasing TIT, followed by the corresponding increase in OPR. In addition, increasing TIT results in larger w, leading to more power-dense cores capable of powering turbofans with large BPR.

The TIT is limited by the working life of the highly stressed components in the first stage of the turbine. The spinning turbine blades are experiencing enormous tensile stress from rotation in combination with a reduction in strength from the high temperatures. Therefore, the blades are cooled using cooling air that is extracted from the cycle before the combustor. Advancements in high-temperature materials and cooling technologies have increased the TIT from 1050 K (Whittle W.1 engine in 1940) to 1800 K seen in modern engines [32]. This has been accompanied by an increase in OPR from 3.14 in the first production jet engine, the 1944 Junkers Jumo 004 [33], to 60 in the General Electric GE9x [34]. An increase in TIT will lead to higher cooling requirements for the turbine, denying some of the efficiency gains. This is amplified by the fact that the cooling air becomes hotter due to the higher compressor outlet temperature due to the increased OPR [35]. In addition, increasing OPR also becomes more difficult, as the high pressure in the final stages of the compressor is accompanied by a higher density of air. Higher density leads to smaller flow path and hence smaller compressor blades. It is harder to make small blades efficient, and losses increase. Together, this leads to the projected thermal efficiency to level out [22] sometime in the future.

This is a fundamental limit of the cycle in which the engine operates. To further make the core more efficient, a new type of thermodynamic cycle is needed [23]. In the next chapter, we will present a promising new concept that offers higher thermal efficiency.

3

Composite cycle engine

The composite cycle engine (CCE) is a novel engine that enables further efficiency gains relative to today's and future best in class turbofans. The baseline architecture of the turbofan is retained, but the core is further enhanced by combining it with a piston engine. To provide the reader with the necessary background to understand the concept, this chapter starts with explaining how piston engines work, in Section 3.1. Thereafter, the composite cycle concept is introduced in Section 3.2. Three technical solutions to implement the concept are described in the following sections. Section 3.3 describes the crankshaft baseline architecture, in Section 3.4 and 3.5 the free-double and opposed piston variants are introduced in 3.5.

3.1 Piston engines

As was explained in the previous chapter, the turbofan core operates on the Joule thermodynamic cycle, where heat is added in the constant pressure burner. One of the main limiting factors is the cycle peak temperature, due to the material limits of the turbine.

The CCE concept targets improvements in the heat addition phase of the cycle, both by increasing the average temperature at which heat is added and by doing so through constant-volume combustion. Constant-volume heat addition is when heat is added to a gas in a fixed volume, such as a sealed cylinder. Because the gas has nowhere to expand, the pressure of the gas rises. Additionally, the temperature rises more for the same added heat relative to the constant pressure counterpart. The reason is again related to the fact that the gas cannot expand, hence all the fuel energy is converted into temperature rise. This is why the constant volume heat capacity is lower than the constant pressure heat capacity. The constant pressure burner, on the other hand, is open,

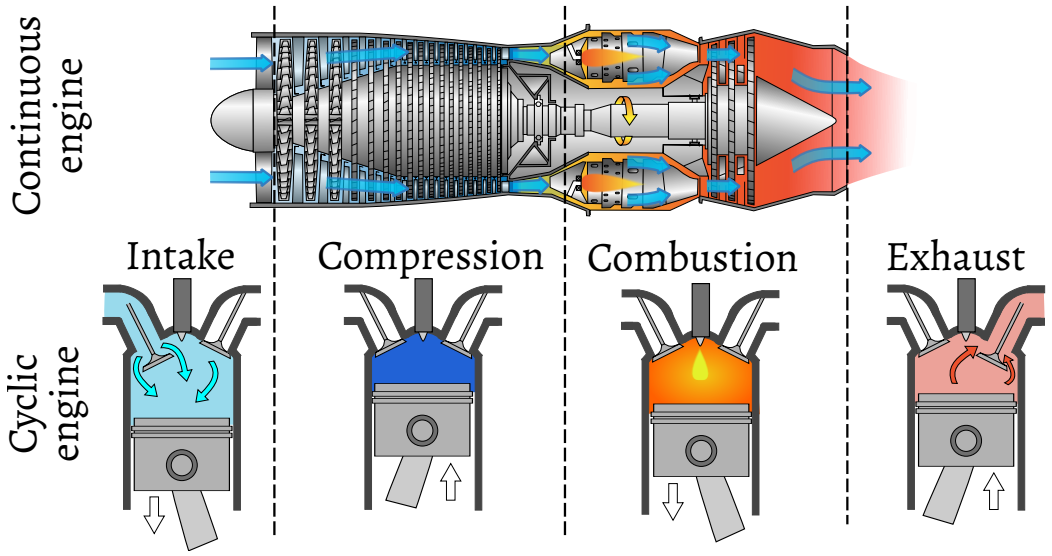

Figure 3.1: Comparison of gas turbine engine and reciprocating engine operation. Adapted from Jet engine by Jeff Dahl, via Wikimedia Commons, CC-BY-SA 4.0.

which does not cause any rise in gas pressure. Constant-volume heat addition is therefore inherently more thermally efficient than constant pressure heat addition.

One way of practically achieving combustion that is partially at constant volume is inside piston engines. A piston engine is also an internal combustion engine, like a gas turbine, but the gas energy is converted into work by reciprocating pistons instead of rotating turbine blades. The working principle of the reciprocating engine is the same as that of the gas turbine, with air intake, compression, combustion, power extraction, and exhaust. A comparison of the two engines is presented in Fig. 3.1, where a four-stroke compression-ignition engine is shown. The reciprocating engine consists of intake and exhaust valves, which can be closed and opened, a piston that can move up and down, and a fuel injector. First, the intake valve is open and the piston moves downwards, filling the cylinder with fresh air. When the intake valve is closed, the piston moves upward, compressing the air and increasing the temperature and pressure. Near the top, when only a small volume remains, fuel is injected into the hot gas. The fuel reacts with the air and autoignites, rapidly increasing temperature and pressure. Due to the increased pressure, the piston moves downward, extracting work from the gas. Finally, the exhaust valve opens and the combustion products are pushed out of the cylinder by the upward motion of the piston. The force on the piston during the expansion after combustion is greater than the force exerted by the piston on the gas during the compression phase, resulting in a net positive work output.

3.2 Composite cycle concept

The main difference between the engines is that the gas turbine is a continuous engine, whereas the piston engine is an intermittent engine. All four processes are occurring simultaneously in the gas turbine, separated spatially. In the piston engine, the operation is cyclic, with all processes taking place in the cylinder but separated temporally. The principal advantage of the continuous engine is the high mass flow rate in relation to the size of its machinery. A high mass flow rate of air allows for a high rate of fuel combustion, leading to high power output and a large power-to-weight ratio. A high power-to-weight ratio is one of the most important metrics of aeroplane propulsion, and this is why gas turbines dominate the field.

Intermittent engines, on the other hand, offer a higher theoretical thermal efficiency. Since combustion takes place faster than the movement of the piston, heat addition results in a pressure increase, which is more similar to constant-volume combustion. In addition, higher peak pressures and temperatures can be achieved because of the cyclic operation of the piston engine. The walls only need to endure the high temperatures for a short period of time before being cooled by the admission of new, cool air.

The rationale for the composite cycle engine is to combine the thermal efficiency of the piston engine with the power density of the gas turbine. Turbomachinery is used to manage large mass flows in the low-pressure part of the power plant, where the gas density is low. For the high-pressure part of the engine, where the air density is higher, a piston engine is used to add heat to the cycle. In that way, the highest pressures and temperatures are seen only in the piston engine. There are multiple technical concepts to realise this cycle, and the three engine architectures being studied in the MINMAL project will be presented below.

3.3 Crankshaft based composite cycle engine

This concept, illustrated in Fig. 3.2 is the one that has been studied in my second paper. It is the most technologically mature concept, but also the heaviest. The air admitted by the engine is first seen by the fan that produces most of the thrust through the cold nozzle. It is connected to the low-pressure shaft via a reduction gearbox . A large part of the air pressurised by the fan bypasses the engine and flows into the bypass duct. The remaining air flows into the core, and is further compressed by the high-speed LPC. After, the intercooler cools the core air using a fraction of the bypass air in an auxiliary bypass duct. The core air is subsequently pressurized by an axial-radial HPC powered by two V12 piston engines via a gearbox. This gearbox is needed since the HPC is rotating at more than 10,000 RPM and the crankshaft of the piston engine at around 2000 RPM. Note that the last stages of the HPC and the entire HPT of a conventional turbofan are replaced by a piston engine. Hence, the CCE gas generator for the crankshaft concept is

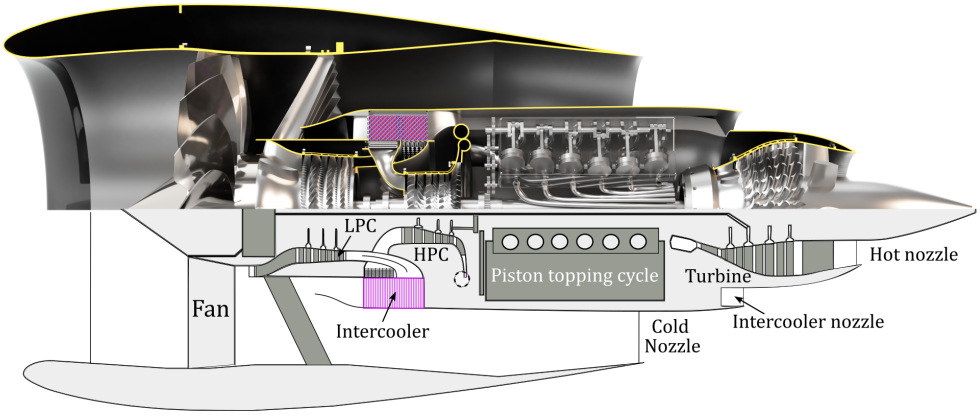

Figure 3.2: A visualisation of the crankshaft CCE concept, with a rendering of the power plant in the upper half and a schematic drawing in the lower half.

composed by the piston engine and the HPC, producing gas power for the subsequent turbine. Downstream of the piston engine is a secondary constant pressure combustor that allows for the production of extra power when needed. The high temperature and high pressure gas is expanded in the turbine that powers both LPC and the fan. Finally, the gas is expanded in the core nozzle to produce thrust. As can be seen in Fig. 3.2, some of the bypass air is diverted into the intercooler, exiting through the intercooler nozzle and also contributing to the production of thrust. The intercooler is beneficial for the cycle by increasing the density of the core air, which reduces the piston engine size. Another benefit is the reduction of NO_x production due to the reduced air temperatures. Not shown here, but the bypass air is also used to cool the piston engine through an oil-air heat exchanger.

In addition to offering benefits from the increase in the thermal efficiency of the core, the CCE is predicted to reduce the climate impact by allowing more flexible in operations. Since contrails contribute approximately to half of the total climate impact of global aviation, avoiding the creation of contrails is an easy measure to reduce their impact. Contrail cirrus only form under certain local atmospheric conditions, and circumventing these regions would result in no clouds forming. That would mean changing the flying altitude to fly above or below the said regions. Gas turbines, however, suffer a great loss in thermal efficiency when operating at part load, outside the design conditions. Compression ignition piston engines do not show the same drop in thermal efficiency at part load since the compression ratio and peak pressure are still relatively high. With variable injection and valve timing, the operation can be further improved. Hence, the CCE can also be implemented for flexible altitude operation with reduced

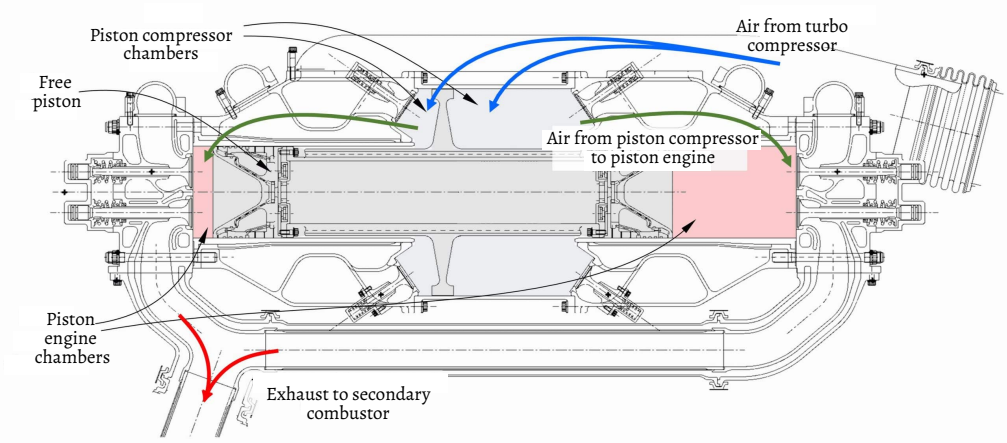

Figure 3.3: The free double piston concept, with the piston in grey in the centre. Combustion chambers are marked in red, with the piston compressor volume shown in blue. Adapted from [36].

fuel consumption relative to conventional turbofan engines.

3.4 Free-double piston

One of the primary concerns of the CCE is the increased weight of the powerplant due to the heavy reciprocating engine. Piston engines partly achieve lower power-to-weight ratios due to the lower mass flow of air, as explained in section 3.2. Another reason is the need to convert the reciprocating force to rotational power, via heavy connecting rods and crankshafts. In the crankshaft based CCE, a gearbox is also needed to connect the HPC to the piston engine, further increasing the weight. In the free-double-piston concept, the crankshaft, connecting rods, gearbox, and HPC are completely removed. This concept was introduced in a 2013 patent by Klingels [28], and a drawing can be seen in Fig. 3.3, adapted from the paper presenting the double piston concept for aero engines [36].

In this concept, a free-piston is used, coloured dark grey and lying horizontally in the figure. Free-piston means it is not mechanically connected via a connecting rod to a crankshaft. Instead, the motion is generated by two combustion chambers, one at each end of the piston, marked red in the figure. Combustion on one side drives the piston towards the other end, where it compresses the air, followed by combustion, and so on. This operating mode is called two-stroke, with combustion occurring each time the piston reaches the top. The exhaust and intake strokes are combined. Fresh air enters the cylinder simultaneously as the exhaust is expelled.

In addition, the HPC is replaced by annular piston compressors. Piston compressors operate with an intake stroke, filling the cylinder with air when the intake valve is open,

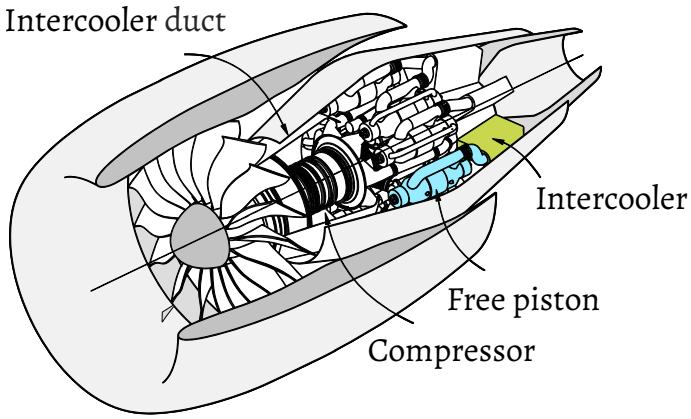

Figure 3.4: Illustration of the free-double piston propulsion system with the engine core visible, figure from [36].

followed by compression of the air by the piston with the valves closed. Air is delivered at higher pressure through the opening of the exhaust valves. The piston compressor chamber is an annulus that surrounds the free-piston. Compression is achieved by the reciprocating motion of the piston, from left to right in Fig. 3.3. The clever design lies in that the piston compressor is directly mounted on the free-piston, leading to a 100% transfer efficiency from the piston engine power to the compressor, with a very light design.

For the free double piston, the lateral forces between the piston and cylinder walls are minimal due to the lack of a connection rod to a rotating shaft. Hence, demands on piston lubrication are therefore reduced, possibly allowing for air-lubrication instead of oil. The wall temperatures could therefore increase substantially beyond the normal limit set by the required oil operating temperature. Also, heat losses from the combustion gas to the walls can be reduced because of the smaller temperature difference between the gas and the wall. Additionally, this would enable using the core air to cool the engine instead of the bypass air, retaining heat losses within the core flow path and increasing its efficiency.

An illustration of the propulsion system with the free-double piston core is shown in Fig. 3.4. The free-piston devices are arranged circumferentially around the secondary combustor, immediately after the compressor. This illustration also includes an intercooler that cools the core air between the axial compressor and piston compressors.

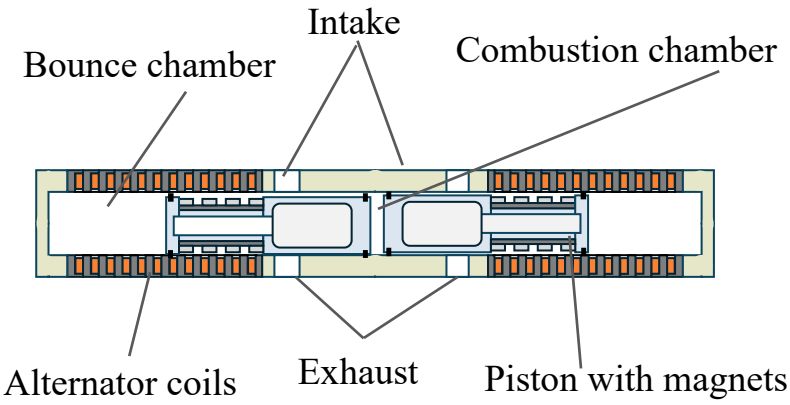

Figure 3.5: Schematic of the opposed free-piston linear alternator. Electricity is generated from the power stroke of the pistons equipped with magnets. Figure by A.Rolt, from presentation by A.Seitz [37].

3.5 Opposed piston

The third and final CCE concept studied in the MINIMAL project uses an opposed free-piston arrangement. In Fig. 3.5, the opposed piston engine is shown. This piston engine arrangement also operates without a crankshaft. Two free pistons are placed in an opposed arrangement, meaning that they are reciprocating against each other. Power is generated with alternator coils and magnets, which generate electrical power rather than mechanical power. The motion of the piston can therefore also be controlled electrically, offering great operational flexibility. This benefit is used in the proposed concept by operating with homogeneous charge compression ignition, an advanced combustion mode. This means that fuel and air are mixed outside the cylinder, creating a homogeneous lean mixture. This mixture is then compressed until it autoignites. The concept has been well researched before and offers the thermal efficiency benefit of compression ignition but at the cost of very low levels of NO_x, because it can operate very lean, with no parts of the mixture close to stoichiometric conditions. However, it is known to be very hard to control, as autoigniton must occur at precisely the right time. The concept of electrically controlled piston movement may be a solution to this. Another benefit of the opposed piston arrangement is the lack of vibrations due to the forces cancelling out. Experimental work on this concept is carried out at Cranfield University, where the objective is to demonstrate low-NO_x operation.

4

Modelling

The workings of both gas turbine engines and piston engines are, of course, very complex. One could devote an entire PhD (or career) to studying one of the many components that comprise these advanced machines. My job, however, is not to look at any individual component in detail, but rather at the system that is created from the combination of all these components. Therefore, I will not be using any method that could be called ”state-of-the-art”. Rather, the methods that I have been using are often simple. The goal has been to find methods that model certain phenomena to a sufficient level of detail, preferably in the simplest way possible. With this approach, I have been able to build a system model that captures the fundamental behaviour of the CCE.

This chapter presents the most important models that have been used in the analysis of the CCE. More detailed descriptions of the modelling are presented in both papers. The first paper explains in detail the piston engine performance modelling, whereas the second paper presents the modelling framework for NO_x production and the system model.

First, in Section 4.1 the core of the entire framework is presented: the properties of the working fluids. In Section 4.2, the modelling of the turbomachinery is presented. From an aviation perspective, the most unique component in the CCE is the piston engine, which is given two sections. Section 4.3 describes how the thermodynamic performance of the reciprocating engine is modelled. Subsequently, Section 4.4, is dedicated to the modelling of NO_x production. The chapter is concluded with a presentation of how all the different models are connected in a system model, in Section 4.5.

4.1 Thermodynamic properties

All gases are modelled as semi-perfect gases, meaning they are governed by the ideal gas law but the heat capacities are temperature dependent. The ideal gas law can be written as:

$$pV = mRT, \tag{4.1}$$

with p being the pressure of the gas, V the volume, m the mass, R the specific gas constant, and T the temperature. Fluid properties are modelled with the NASA Glenn coefficients [38], which are obtained from the library used in the NASA CEA (Chemical Equilibrium with Applications) computer programme [39]. Thermodynamic properties of individual species are represented as temperature polynomials, with mass specific heat capacities, c_p, expressed as:

$$\frac{c_P(T)}{R} = a_1 T^{-2} + a_2 T^{-1} + a_3 + a_4 T + a_5 T^2 + a_6 T^3 + a_7 T^4, \tag{4.2}$$

where a_i are the coefficients. Two different sets of coefficients are specified for the temperature ranges $200\,\mathrm{K} < T < 1000\,\mathrm{K}$ and $1000\,\mathrm{K} < T < 6000\,\mathrm{K}$. Furthermore, the specific enthalpy, h, and the standard entropy, s°, at the reference pressure, $p^\circ = 1$ bar, are obtained by integration and are defined as:

$$\begin{aligned} \frac{h(T)}{RT} &= \frac{1}{RT}\left[\Delta_f h^\circ_{298K} + \int_{298.15}^{T} c_p(T)dT\right] \\ &= -a_1 T^{-2} + a_2 \frac{\ln T}{T} + a_3 + \frac{a_4 T}{2} + \frac{a_5 T^2}{3} + \frac{a_6 T^3}{4} + \frac{a_7 T^4}{5} + \frac{b_1}{T}, \end{aligned} \tag{4.3}$$

and

$$\begin{aligned} \frac{s^\circ(T)}{R} &= \frac{1}{R}\int_0^T \frac{c_p(T)}{T}dT \\ &= -\frac{a_1 T^{-2}}{2} - a_1 T^{-1} + a_3 \ln T + a_4 T + \frac{a_5 T^2}{2} + \frac{a_6 T^3}{3} + \frac{a_7 T^4}{4} + b_2, \end{aligned} \tag{4.4}$$

where $\Delta_f h^\circ_{298K}$ is the heat of formation at 298.15 K and b_i are integration constants. The entropy at any other pressure, p, is obtained from:

$$s(T, p) = s^\circ(T) - R \ln\left(\frac{p}{p^\circ}\right). \tag{4.5}$$

Further, the properties of a mixture, e.g. air or combustion products, are calculated by summing the individual species' properties weighted by their mass fraction.

The air is assumed to be completely dry and to have the molar composition of 78.1 % N_2, 21.0 % O_2 and 0.9 % Ar. In this thesis, two types of fuel are considered, hydrogen

H_2, and Jet A, here modelled as $C_{12}H_{23}$. The ideal combustion of the reactants is given by the corresponding reactions, ignoring the inert gases, for Jet A:

$$\begin{aligned} \phi \cdot C_{12}H_{23} + 17.75 \cdot O_2 \\ \rightarrow 12 \cdot \phi \cdot CO_2 + 11.5\phi \cdot H_2O + 17.75 \cdot (1-\phi) \cdot O_2, \end{aligned} \tag{4.6}$$

and for H_2:

$$\begin{aligned} \phi \cdot H_2 + 0.5 \cdot O_2 \\ \rightarrow \phi \cdot H_2O + 0.5 \cdot (1-\phi) \cdot O_2, \end{aligned} \tag{4.7}$$

where $\phi = \frac{f}{f_s}$ is the fuel-air-equivalence ratio. It is the ratio of combusted fuel-air ratio, f, to the stoichiometric fuel-air ratio, f_s. From the thermodynamic data and the ideal reactions, the lower heating value, Q_{net}, of Jet A amounts to 43.0 MJ kg^{-1} and for H_2 it becomes 120.0 MJ kg^{-1}. Further, we have $f_s = 0.0681$ for Jet A and $f_s = 0.0292$ for H_2.

4.2 Turbomachinery

The essential components of the gas turbine are the compressors and turbines. Thermodynamically, the turbomachinery is modelled as sequences of adiabatic compressions and expansions. Compression in a compressor is described with a prescribed pressure ratio between the outlet and inlet, $p_2/p_1 = \Pi_c$. The efficiency with which this increase in pressure is achieved is quantified by the polytropic efficiency, η_c. Less efficient compression means that the temperature increases more, resulting in more power needed to drive the compressor. The outlet temperature, T_2, is found by combining the definition of polytropic efficiency:

$$\eta_c = \frac{dT_s}{dT}, \tag{4.8}$$

where dT_s is the temperature increase of an isentropic compression, with the entropy differential for an isentropic process:

$$ds = \frac{c_p}{T} dT_s - R\frac{dp}{p} = 0. \tag{4.9}$$

Together, the following relation between Π_c, η_c and s° is obtained:

$$\ln \frac{p_2}{p_1} = \frac{\eta_c}{R} \int_{T_1}^{T_2} \frac{c_p}{T} dT = \frac{\eta_c}{R}(s^\circ(T_2) - s^\circ(T_1)) = \ln \Pi_c, \tag{4.10}$$

where T_2 is found from the iteration of the entropy polynomial. For a given mass flow rate, $\dot{m}$, the required compression power, P_c, is found from:

$$P_c = \dot{m} \left[h(T_2) - h(T_1) \right], \tag{4.11}$$

where h is the mass specific enthalpy.

The expansion in the turbine is modelled with a given turbine power extraction, P_t, which together with the mass flow, $\dot{m}$, gives the outlet enthalpy, h_2, from the power balance:

$$h_2 = h_1 - \frac{P_t}{\dot{m}}. \tag{4.12}$$

The turbine is modelled with an isentropic efficiency, η_t, which quantifies how much pressure drops to generate the required power. More efficient turbines produce more power with a lower pressure ratio. Using the definition of isentropic efficiency:

$$h(T_{2,s}) = h_1 - \frac{h_1 - h_2}{\eta_t}, \tag{4.13}$$

the isentropic outlet temperature, $T_{2,s}$, is found. By finding which pressure would result in a state with the same entropy as the turbine inlet:

$$s(T_{2,s}, p_2) = s(T_1, p_1), \tag{4.14}$$

the outlet pressure, p_2 can be calculated.

4.3 Piston engine performance

From a performance point of view, the main metrics of interest for the piston engine are power output, heat losses, air mass flow, engine size, outlet temperature, and peak pressure. The simplest and most computationally cheap method of modelling these is with a zero-dimensional model. The model treats the cylinder volume as a single control volume, which means that the gas properties have one single value throughout the cylinder. By varying the volume, adding heat, exchanging gas, and transferring heat through the boundaries, the working cycle of the piston engine is simulated. A visualisation of the model is shown in Fig. 4.1. The control volume is shown as the dotted area, with state variables mass, m, temperature, T, volume, V, pressure, p and fuel-air-equivalence ratio, ϕ. The model has been implemented as explained in the technical NASA report by Van Gerpen [40].

In Fig. 4.1 the energy flows are shown in green, with the addition of heat from fuel Q_f, pressure work W, and heat losses through the volume boundaries: cylinder head, Q_{head}, cylinder walls, Q_{wall} and piston Q_{piston}. The mass flow is represented by blue arrows and enters through the intake, m_i, with the fuel, m_f and exits through the exhaust, m_e. With the transfer of mass, there is also a corresponding transfer of enthalpy, H, shown with red arrows.

The principal governing equation is the ideal gas law, which is differentiated with respect to time to obtain the temporal evolution of the system variables:

$$p\dot{V} + \dot{p}V = mR\dot{T} + m\dot{R}T + \dot{m}RT, \tag{4.15}$$

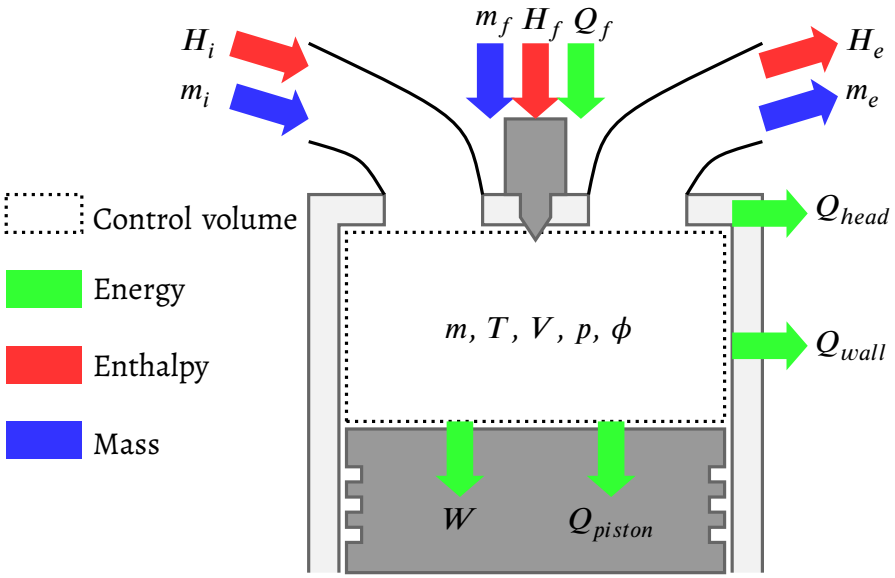

Figure 4.1: Piston model drawing showing the combustion chamber control volume and the mass, enthalpy and energy flows.

with the dot denoting the change with respect to time. Further, the conservation of energy of the system is written as:

$$\dot{U} = \dot{Q} - \dot{W} + h_i \dot{m}_i - h_e \dot{m}_e + h_f \dot{m}_f, \tag{4.16}$$

where U represents the internal energy of the system, Q the heat supplied to the system, W the work performed by the system, and h the specific enthalpy. The subscripts i, e and f denote the flow across the intake, exhaust, and fuel injector.

The change in system volume is driven by a prescribed reciprocating motion of the piston, which can be expressed as a function of the rotation angle of the crankshaft, θ, where one revolution of the shaft results in a sweep of the volume of the entire piston. The total variation in the volume of the cylinder with θ is expressed as [41]:

$$V(\theta) = V_d \left[\frac{1}{\epsilon - 1} + \frac{1 - \cos\theta}{2} + \frac{s}{16 \cdot l_{con}} (1 - \cos(2\theta)) \right], \tag{4.17}$$

where ϵ is the geometric compression ratio, s the stroke, and l_{con} the length of the connecting rod.

To close the system of equations, sub-models are needed for mass flow through the valves, heat addition from combustion, and heat transfer to the walls. Mass flow is modelled as an isentropic expansion of a gas between two reservoirs of different pressure. A prescribed mass of fuel is combusted, deciding the amount of heat added. The rate of heat addition follows a prescribed curve with three parameters: start of combustion,

θ_{SC}, combustion duration, $\Delta\theta_{CD}$ and shape factor, m_w. Newton's law of cooling is used to model the heat transfer between gas and the walls:

$$\dot{Q}_{w,j} = \alpha \sum_j A_j (T - T_{w,j}), \tag{4.18}$$

where A_j and $T_{w,j}$ are the area and temperature of the wall j, respectively. The heat transfer coefficient, α, is calculated using a semi-empirical formula [42].

Combining all the equations, we obtain a system of ordinary differential equations. These equations are integrated over the entire engine cycle. Multiple iterations of the integrations are performed until the final and initial conditions are the same, since the piston operation is cyclic.

To integrate the results from the piston performance simulation, the time dependent results are averaged. The outlet temperature, T_2, is found by mass-averaging the outlet enthalpy:

$$h(T_2, \phi_2) - \frac{\int h_e dm_e}{\int dm_e} = 0, \tag{4.19}$$

where ϕ_2 is the mass-averaged equivalence ratio in the exhaust. The power output of the piston is calculated from the total pressure work performed on the piston during the cycle divided by the cycle period, Δt_{cycle}:

$$P_i = \frac{\int pdV}{\Delta t_{cycle}}. \tag{4.20}$$

All other outputs are simply time-averaged.

The developed model was cross-validated against simulation data from an example case provided in the technical report that described the model [40]. This is presented in Paper I.

4.4 Nitrogen oxide production

Nitrogen oxides are produced in piston engines during combustion because of high pressures and temperatures. The production of nitrogen oxides is relatively slow and is sensitive to the local oxygen content and temperature. This means that the reactions need to be modelled with chemical kinetics and a model that captures the local temperature and oxygen content inside the cylinder. Since this model is explained in detail in the second paper, a brief description will be given here. A more detailed description of the chemical kinetics framework is given, in order to expand a bit further on the paper.

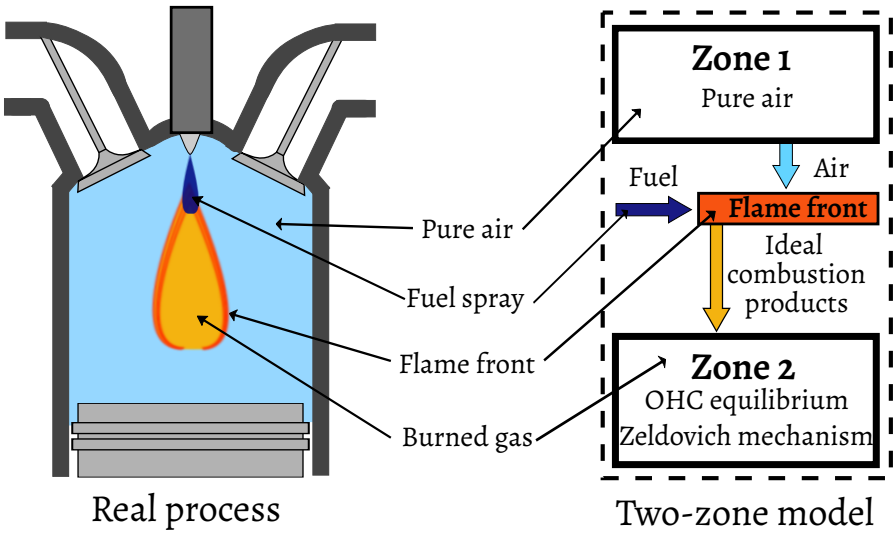

Figure 4.2: A visualisation of direct injection compression ignition combustion together with the two-zone model.

4.4.1 Two-zone model

The primary reaction zone of nitrogen oxides in piston engines is behind the flame front. To predict the temperature and gas composition in the reaction zone, a model that divides the combustion chamber into a burned and unburned zone is used. The model was developed by Heider et al. [43] and a visualisation of the model and the real process of direct injection compression ignition combustion is presented in Fig. 4.2. This type of combustion is the mode of operation for diesel engines. During intake and compression, only air is present in the cylinder volume. The air temperature rises, and when fuel is injected into the cylinder, it mixes with air and auto-ignites. This is seen in the figure with the fuel spray and the flame, with the surrounding gas being air. In the model, before combustion, only the cold zone (zone 1 in the figure) exists. During combustion, mass is transferred from the cold zone to the hot zone (zone 2) according to a given stoichiometry. The temperature of the hot zone initially is close to the flame temperature for that stoichiometry and thereafter gradually decreases. For the calculation of NO_x, it is assumed that reactions occur only in the hot zone. The modelling approach will be described further in the next subsection, explaining the oxygen-hydrogen-carbon (OHC) equilibrium and Zeldovich mechanism shown in the figure.

4.4.2 Chemical kinetics of nitric oxide

Nitrogen oxide, NO_x, is shorthand for the nitrogen oxides that are most relevant for air pollution: nitric oxide, NO and nitrogen dioxide, NO_2. Even if both NO and NO_2 are produced in piston engines, production is dominated by NO and it is most common to model only the production of NO [44]. However, note that NO later will convert to NO_2 in the exhaust system and in the atmosphere. In piston engines, NO can be formed in three ways: thermal NO, prompt NO, and fuel NO. The last type of nitric oxide is only produced from fuel bound nitrogen, for example, in coal. When combusting kerosene, only the thermal and prompt pathways are relevant. Prompt NO develops in the flame front, whereas thermal NO is formed behind the flame front among the hot combustion products. Of these two, the thermal reaction produces around 90% of the total NO, and according to the most common approach in the literature, we will consider only the thermal pathway. Thermal NO is produced by oxidation of diatomic nitrogen and can be represented by the extended Zeldovich mechanism:

$$O^{\bullet} + N_2 \xrightarrow{k_1} NO + N^{\bullet}, \tag{4.21}$$

$$N^{\bullet} + O_2 \xrightarrow{k_2} NO + O^{\bullet}, \tag{4.22}$$

$$N^{\bullet} + OH \xrightarrow{k_3} NO + H^{\bullet}. \tag{4.23}$$

Here, k_1, k_2 and k_3 are the forward reaction rate coefficients, obtainable from chemical kinetics mechanism libraries. Due to the stable triple bond of N_2, the mechanism is relatively slow, limited by reaction (4.21). The reaction rates are of the same order as the physical time scales of the piston engine, which means that the chemical equilibrium cannot be assumed [45]. Due to the forward reactions (4.22) and (4.23) being orders of magnitude faster than (4.21), the N produced in the first reaction is immediately converted in the second and third reaction, and the concentration of atomic nitrogen can therefore be assumed to be quasi-steady:

$$\frac{d[N]}{dt} \approx 0. \tag{4.24}$$

Combining reactions (4.21) - (4.23) with the quasi-steady approximation, one obtains the following equation for the change in nitric oxide concentration:

$$\frac{d[NO]}{dt} = 2\,k_1\,[O]\,[N_2] - 2\,k_{1,r}\,[NO]\,[N], \tag{4.25}$$

and the concentration of atomic nitrogen given by:

$$[N] = \frac{k_1\,[O]\,[N_2] + k_{2,r}\,[NO]\,[O] + k_{3,r}\,[NO]\,[H]}{k_{1,r}\,[NO] + k_2\,[O_2] + k_3[OH]}, \tag{4.26}$$

where the reverse reaction rates have the subscript r. These are calculated with the equilibrium constant, K_c, determined by the difference in free Gibb's energy of the corresponding reactions. Lastly, the concentration of oxygen atoms, [O], is calculated from the OHC-system, Eqs. (4.27) - (4.31).

$$\mathrm{H_2} \longrightarrow 2\,\mathrm{H}, \tag{4.27}$$

$$\mathrm{O_2} \longrightarrow 2\,\mathrm{O}, \tag{4.28}$$

$$\mathrm{H_2O} \longrightarrow \frac{1}{2}\,\mathrm{H_2} + \mathrm{OH}, \tag{4.29}$$

$$\mathrm{H_2O} \longrightarrow \frac{1}{2}\,\mathrm{O_2} + \mathrm{H_2}, \tag{4.30}$$

$$\mathrm{CO_2} \longrightarrow \mathrm{CO} + \frac{1}{2}\,\mathrm{O_2}. \tag{4.31}$$

These reactions are orders of magnitude faster than the Zeldovich mechanism, and thus chemical equilibrium can be assumed [46], with the equilibrium concentrations obtained from Cantera [47]. To obtain the amount of NO produced in the piston engine, Eq. (4.25) is integrated inside the reaction zone of the two-zone model, from the start of combustion until the opening of the exhaust valves.

The developed NO_x model was validated against publicly available experimental data from a diesel engine, with data available in [48]. The results of this validation are presented in Paper II.

4.5 System model

The ultimate goal of the work presented in this thesis is to investigate the behaviour and design considerations of the CCE. To achieve this, all the different models are combined in one system model, simulating the engine. The calculations follow the flow of air inside the engine, where the gas properties are calculated at all stations between the components. A schematic of the CCE model, together with a conceptual design, is shown in Fig. 4.3. Each station is represented with a number, which is shown both in the model schematic and in the drawing. At these stations, the gas pressure, temperature, and composition are calculated. The simulation starts in the ambient atmosphere and progresses from the intake all the way to the propelling nozzles. Each component is represented with a module, which connects with other modules according to the connections shown in the figure. Conservation of mass and energy is ensured between the components. The mass flow of gas is shown with the thin connections, showing the flow paths. Mechanical power is transmitted through shafts and gearboxes, represented by thick lines. Finally, heat is transferred between the modules and flows through heat exchangers, which are visualised by the arrows.

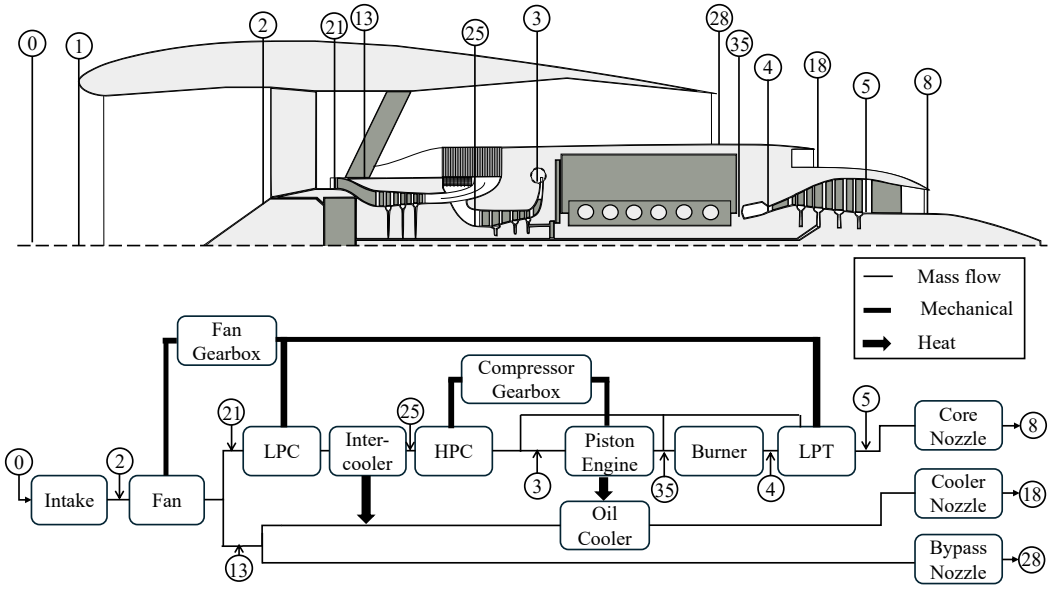

Figure 4.3: A schematic of the studied CCE concept, with a conceptual design of the power plant in the upper half and a visualisation of the system model in the lower half.

The principal output of the model is the thrust, calculated from the gas condition in the nozzles, with the inlet mass flow and ambient conditions as input variables. The key cycle parameters and metrics are also outputs, such as how much fuel was needed to produce the thrust or the amount of NO_x produced. When analysing a specific application, thrust requirements, flight altitude, and speed are often given. To compare with a reference engine, the fan diameter and fan pressure ratio are often fixed, setting the inlet mass flow. The variables inside the engine can then be varied to analyse changes in metrics such as thermal efficiency, propulsive efficiency, NO_x emissions, and piston engine size.

In conclusion, the components of the CCE have been modelled with a variety of models. They have been integrated to simulate the entire propulsion system. This is the model used for the parametric study in Paper II.

5

Conclusions and Outlook

This thesis marks the halfway point of my PhD studies. Most of this time has been spent on model development. For me personally, it has been two instructive years in which I have learnt a lot about aircraft engines, piston engines, thermodynamics, hydrogen, technology development, chemistry, and computational modelling. In the future, the goal is to apply the developed models to learn more about different CCE configurations and NO_x mitigation techniques. In this chapter, a summary of my contributions will be given, based on the results from the two papers. The chapter and the thesis will be concluded with an outlook.

5.1 Summary of results

In my two papers, a modelling framework of the CCE has been presented. This framework was used in Paper II to investigate the design trades of the main engine design variables on performance and NO_x emissions. The trades presented are valuable as they normally are investigated when a new engine concept is to be built. Previously, optimal engine designs have been presented with respect to fuel consumption. However, to learn the effect of the design variables on NO_x, parametric studies are needed. This helps to establish the design space and enables a more straightforward path for the subsequent engine optimisation for minimum climate impact rather than fuel burn.

The results of the parametric study show expected trends, where loading the piston engine core more results in higher efficiency and more NO_x. The OPR of the turbomachinery is limited by the maximum pressure inside the piston engine. For a fixed OPR, an optimum geometric compression ratio of the piston engine was found. Quite surprisingly, at high operating pressures and temperatures, NO_x production was found to be rather insensitive to a further increase in the compression ratio, due to the rather

mild increase in maximum flame temperatures. The specific power output of the piston engine decreased with a lower compression ratio, which means that the size of the piston engine grows with lower compression. This is a limiting factor, since the engine cannot be too large. Intercooling has also been found to have the expected effect, with a smaller piston engine, lower thermal efficiency, and lower NO_x as a result.

To conclude, performance wise, adding as much heat as possible in the piston engine is beneficial. The limiting factors are the size of the piston engine and the maximum pressure. From the perspective of NO_x, the opposite is true, since the piston engine produces the bulk of NO_x.

One of the main takeaways from the results in the second paper is that the CCE operating with compression ignition produces prohibitive levels of NO_x. It produces roughly five times the amount of NO_x compared to a turbofan engine. No single design variable that was changed could reduce the emissions to acceptable amounts. In addition, no parameter was found to increase efficiency and reduce NO_x. To model NO_x production, the simplest form of modelling framework was used, so the results are associated with uncertainties. However, even if the results were to overpredict the emissions by 100%, the emissions would still be too large. These results were not surprising, as diesel engines are known to produce large emissions of NO_x.

As we saw in the introduction, the climate impact of NO_x from global aviation is approximately half that of CO_2. It becomes quite evident then that releasing 10% less CO_2 but releasing five times more nitrogen oxides would only impact the climate more. Hence, to make this concept viable, some kind of NOx-mitigation technology needs to be used.

This study will hopefully help the design of CCE and point in the right direction for further development. It has been evident that NO_x emissions seem to be a big challenge for these kinds of engines.

5.2 Outlook

Based on the findings in Paper II, focusing on techniques to reduce NO_x is the way forward. Concepts such as exhaust gas recirculation, steam injection and valve timing could be studied. In addition, more advanced combustion methods, such as homogeneous charge compression ignition, or premixed charge compression ignition, could be another way to decrease NO_x. Comparing these methods while connecting the model with a climate impact model will be instructive and will allow one to determine the impact of the investigated parameters and aforementioned NO_x mitigation techniques directly on the global average temperature response. In this way, engines can be optimised during their design phase for minimum climate impact, which is quite novel. After that, I could investigate how the CCE would operate on hydrogen, since the performance model is already in place. Perhaps broadening my scope to compare the CCE

with other engine concepts would also be interesting. In reality, there is no silver bullet to ensure climate neutrality in aviation, and most likely not one but various combinations of technologies will be required in the future. The CCE has great potential, but large NO_x reductions must still be demonstrated. *This is what I will do next!*

6

Summary of papers

Paper I

Modelling a hydrogen fuelled composite cycle aero engine

In this paper, the performance modelling framework is presented. First, the piston engine model is described in detail, presenting all sub-models and how the variation of internal energy with respect to fuel-air-equivalence ratio is handled. A satisfactory cross-validation against simulation data is performed. In addition, the operation of piston engines on hydrogen is discussed. The paper is concluded with a successful validation against experimental data on the operation of the piston engine on hydrogen.

Paper II

Analysis of NOx emissions and thermodynamic cycle performance of a composite cycle aero engine

This paper followed on the first one by adding the modelling of nitrogen oxide emissions. The implemented two-zone model is described in detail. A validation of NO emissions against experimental data is presented. The results of the simulation of the entire composite cycle engine were presented. A parametric study is performed showing trends in thermal efficiency, power density, and NO_x by varying key cycle variables. No variable was found to increase efficiency and reduce NO_x simultaneously. Without any NO_x-mitigation strategy, the composite cycle engine produces significantly higher nitrogen oxide emissions than the reference engine.

Bibliography

[1] H. H. Thorp, *Here comes the Sun,* Science **390**, 1195 (2025).

[2] Ember, *Highlights of the global energy transition in 2025,* Available at: https://ember-energy.org/latest-insights/highlights-of-the-global-energy-transition-in-2025/ (accessed 2026-01-31), 2025.

[3] L. D S, F. D W, S. A, A. M R, B. U, C. Q, D. S J, F. S, F. P M, F. J, G. A, D. R R, L. L L, L. M T, M. R J, O. B, P. J E, P. G, P. M J, S. R, and W. L J, *The contribution of global aviation to anthropogenic climate forcing for 2000 to 2018,* Atmospheric Environment **244**, 117834 (2021). doi:https://doi.org/10.1016/j.atmosenv.2020.117834.

[4] C. J. Smith, R. J. Kramer, G. Myhre, K. Alterskjær, W. Collins, A. Sima, O. Boucher, J.-L. Dufresne, P. Nabat, M. Michou, *et al.*, *Effective radiative forcing and adjustments in CMIP6 models,* Atmospheric Chemistry and Physics **20**, 9591 (2020).

[5] J. Rogelj, M. Schaeffer, M. Meinshausen, D. T. Shindell, W. Hare, Z. Klimont, G. J. Velders, M. Amann, and H. J. Schellnhuber, *Disentangling the effects of CO2 and short-lived climate forcer mitigation,* Proceedings of the National Academy of Sciences **111**, 16325 (2014).

[6] M. Sharmina, O. Y. Edelenbosch, C. Wilson, R. Freeman, D. Gernaat, P. Gilbert, A. Larkin, E. Littleton, M. Traut, D. Van Vuuren, *et al.*, *Decarbonising the critical sectors of aviation, shipping, road freight and industry to limit warming to 1.5–2 C,* Climate Policy **21**, 455 (2021).

[7] A. H. Epstein and S. M. O'Flarity, *Considerations for reducing aviation's co 2 with aircraft electric propulsion,* Journal of Propulsion and Power **35**, 572 (2019).

[8] AIN Media Group, *Heart Aerospace Advances Plans for ES-19 Electric Regional Airliner,* https://www.ainonline.com/news-article/2020-09-23/heart-aerospace-advances-plans-es-19-electric-regional-airliner, (accessed 2026-01-30), 2020.

[9] M. Wise, M. Muratori, and P. Kyle, *Biojet fuels and emissions mitigation in aviation: An integrated assessment modeling analysis,* Transportation Research Part D: Transport and Environment **52**, 244 (2017). doi:https://doi.org/10.1016/j.trd.2017.03.006.

[10] C. Bergero, G. Gosnell, D. Gielen, S. Kang, M. Bazilian, and S. J. Davis, *Pathways to net-zero emissions from aviation,* Nature Sustainability **6**, 404 (2023).

[11] P. Bardon and O. Massol, *Decarbonizing aviation with sustainable aviation fuels: Myths and realities of the roadmaps to net zero by 2050,* Renewable and Sustainable Energy Reviews **211**, 115279 (2025). doi:https://doi.org/10.1016/j.rser.2024.115279.

[12] S. Brynolf, J. Hansson, J. E. Anderson, I. R. Skov, T. J. Wallington, M. Grahn, A. D. Korberg, E. Malmgren, and M. Taljegård, *Review of electrofuel feasibility—prospects for road, ocean, and air transport,* Progress in Energy **4**, 042007 (2022). doi:10.1088/2516-1083/ac8097.

[13] X. S. Zheng and D. Rutherford, *Fuel burn of new commercial jet aircraft: 1960 to 2019,* Int Counc Clean Transp: Washington, DC, USA , (2020).

[14] J. J. Lee, S. P. Lukachko, I. A. Waitz, and A. Schafer, *Historical and future trends in aircraft performance, cost, and emissions,* Annual Review of Energy and the Environment **26**, 167 (2001).

[15] Smithsonian, *Rolls-Royce Conway RCo.12 Mark 509 Turbofan Engine,* https://airandspace.si.edu/collection-objects/rolls-royce-conway-rco12-mark-509-turbofan-engine/nasm_A19870225000, (accessed 2026-01-31), 2026.

[16] MTU Aero Engines, *Pratt & Whitney GTF engine,* https://www.mtu.de/engines/commercial-aircraft-engines/narrowbody-and-regional-jets/gtf-engine-family/, (accessed 2026-01-31), 2026.

[17] T. Grönstedt, C. Xisto, V. Sethi, A. Rolt, N. Roas, A. Seitz, D. Misirlis, J. Whurr, N. Tantot, M. Dietz, *et al.*, *Conceptual design of ultra-efficient cores for mid-century aircraft turbine engines,* in *Proceedings of the 24th ISABE Conference, Canberra, Australia*, 22, 2019.

[18] R. Kirner, L. Raffaelli, A. Rolt, P. Laskaridis, G. Doulgeris, and R. Singh, *An assessment of distributed propulsion: Advanced propulsion system architectures for conventional aircraft configurations,* Aerospace Science and Technology **46**, 42 (2015).

[19] CFM International, *RISE Program: Revolutionary Innovation for Sustainable Engines,* https://www.cfmaeroengines.com/rise, (accessed 2026-01-28), 2026.

[20] D. Smith, A. Filippone, and N. Bojdo, *Noise reduction of a counter rotating open rotor through a locked blade row,* Aerospace Science and Technology **98**, 105637 (2020).

[21] L. S. Langston, *Aspects of gas turbine thermal efficiency,* Mechanical Engineering **142**, 54 (2020).

[22] K. S, S. A, V. P, and H. M, *Unified thermodynamic evaluation of radical aero engine cycles,* in *Proceedings of ASME Turbo Expo 2016*, GT2016-56313, (Seoul, South Korea), 2016.

[23] J. Kurzke, *Achieving maximum thermal efficiency with the simple gas turbine cycle,* Google Scholar, 2003.

[24] T. Grönstedt, C. Xisto, V. Sethi, A. Rolt, N. García Rosa, A. Seitz, K. Yakinthos, S. Donnerhack, P. Newton, N. Tantot, *et al.*, *Ultra low emission technology innovations for mid-century aircraft turbine engines,* in *Turbo Expo: Power for Land, Sea, and Air*, vol. 49743, V003T06A001, American Society of Mechanical Engineers, 2016.

[25] F. Global, *Napier Nomad-An Engine of Outstanding Efficiency,* Flight Global **4**, 543 (1954).

[26] S. James, *World Encyclopedia of Aircraft Manufacturers: From the Pioneers to the Present Day (2nd edition),* Reference Reviews **20**, 46 (2006). doi:10.1108/09504120610655619.

[27] J. Whurr, *Aircraft compound cycle propulsion engine,* 1997.

[28] H. Klingels, *Wärmekraftmaschine Mit Freikolbenverdichter,* European Patent EP2650510 A **2**, 2013 (2013).

[29] S. Kaiser, M. Nickl, C. Salpingidou, Z. Vlahostergios, S. Donnerhack, and H. Klingels, *Investigations of the synergy of Composite Cycle and intercooled recuperation,* The Aeronautical Journal **122**, 869 (2018).

[30] S. Kaiser, *Multidisciplinary Design of Aeronautical Composite Cycle Engines*. PhD thesis, Technische Universität München, 2020.

[31] H. I. H. Saravanamuttoo, G. F. C. Rogers, and H. Cohen, *Gas turbine theory* (Pearson education, 2001).

[32] L. Xu, S. Bo, Y. Hongde, and W. Lei, *Evolution of Rolls-Royce air-cooled turbine blades and feature analysis,* Procedia Engineering **99**, 1482 (2015).

[33] S. Farokhi, *Aircraft Propulsion: Toward Net-Zero Aviation* (John Wiley & Sons, 2025).

[34] Federal Aviation Administration, *Type Certificate Data Sheet E00095EN,* https://drs.faa.gov/browse/excelExternalWindow/DRSDOCID1144837364202302031810020001?modalOpened=true, (accessed 2026-01-30), 2023.

[35] J. H. Horlock, D. T. Watson, and T. V. Jones, *Limitations on Gas Turbine Performance Imposed by Large Turbine Cooling Flows,* Journal of Engineering for Gas Turbines and Power **123**, 487 (2001). doi:10.1115/1.1373398.

[36] S. Kaiser, O. Schmitz, and H. Klingels, *Aero engine concepts beyond 2030: Part 2—the free-piston composite cycle engine,* in *Turbo Expo: Power for Land, Sea, and Air*, vol. 84140, V005T06A018, American Society of Mechanical Engineers, 2020.

[37] A. Seitz, *Composite Cycle Engine Design for Minimal Climate Impact – Study Setup & Reference Systems,* in *Proceedings of the 13th EASN International Conference*, (Salerno, Italy), 2023.

[38] M. B. J, Z. M. J, and G. S, *NASA Glenn coefficients for calculating thermodynamic properties of individual species,* tech. rep., Glenn Research Center, Cleveland, Ohio, 2002.

[39] S. Gordon and B. J. McBride, *Computer program for calculation of complex chemical equilibrium compositions and applications,* tech. rep., NASA Lewis Research Center, Cleveland, Ohio, 1996.

[40] V. J. H., *A two-stroke diesel engine simulation program,* tech. rep., Engine Research Institute, Iowa State University, Ames, Iowa, 1990.

[41] M. GP, T. R, *et al.*, *Grundlagen Verbrennungsmotoren* (Springer, 2014).

[42] H. G. F, *Advanced Approaches for Heat Transfer Calculations,* SAE Transactions **88**, 2788 (1979). http://www.jstor.org/stable/44699090.

[43] G. Heider, G. Woschni, and K. Zeilinger, *2-Zonen Rechenmodell zur Vorausrechnung der NO-Emission von Dieselmotoren,* MTZ - Motortechnische Zeitschrift **59**, 770 (1998). doi:10.1007/BF03226479.

[44] P. Eyzat and J.-C. Guibet, *A new look at nitrogen oxides formation in internal combustion engines,* SAE Transactions , 481 (1968).

[45] S. Shahed and H. Newhall, *Kinetics of nitric oxide formation in propane-air and hydrogen-air-diluent flames,* Combustion and Flame **17**, 131 (1971).

[46] H. Newhall and S. Shahed, *Kinetics of nitric oxide formation in high-pressure flames,* Symposium (International) on Combustion **13**, 381 (1971). doi:https://doi.org/10.1016/S0082-0784(71)80041-3.

[47] D. G. Goodwin, H. K. Moffat, I. Schoegl, R. L. Speth, and B. W. Weber, *Cantera: An Object-oriented Software Toolkit for Chemical Kinetics, Thermodynamics, and Transport Processes,* https://www.cantera.org, 2025. doi:10.5281/zenodo.17620923.

[48] C. Rakopoulos, D. Rakopoulos, and D. Kyritsis, *Development and validation of a comprehensive two-zone model for combustion and emissions formation in a di diesel engine,* International journal of energy research **27**, 1221 (2003).